RSC Advances

ROYAL SOCIETY OF CHEMISTRY

www.rsc.org/advances

Ag-decorated ZnO nanorods prepared by photochemical deposition and their high selectivity to ethanol using conducting oxide electrodes

Can Suo, Chaojun Gao, Xuyang Wu, Yan Zuo, Xinchang Wang, Jianfeng Jia*

A novel gas sensor structure is presented in this work. It consists of $LaNiO_3$ thin film electrodes and gas sensitive Ag nanoparticle-decorated ZnO nanorods. ZnO nanorods were successfully synthesized by a facile wet chemical method in aqueous solution at 95 °C, and then the ZnO nanorods were decorated with Ag NPs through photochemical deposition. Dielectrophoresis was used to position the Ag-decorated ZnO nanorods on the $LaNiO_3$ electrodes. The as-prepared devices combined the advantages of one-dimensional nanostructure, highly ordered array, the chemical stability of the electrode and Ag decoration, which resulted in a dramatically sensing performance for gas detection. The as-prepared gas sensors have definitely high selectivity to ethanol, besides of the improvememt of response and recover speeds.

Key words: ZnO nanorods; Ag nanoparticles decoration; Photochemical deposition; Conducting metal oxide; Dielectrophoresis (DEP); Gas sensing

1. Introduction

Recently, one-dimensional nanostructures have received considerable attention due to their unique physical, chemical, optical, and electrochemical properties.[1] As a promising semiconductor metal-oxide material, zinc oxide (ZnO) has been considered as ideal building blocks for sensors, photocatalysis, optics and photovoltaic devices due to its wide direct band gap of 3.37 eV and large exaction binding energy of 60 meV at room temperature.[2,3] Various one-dimensional (1D) nanostructures of ZnO

*School of Physical Engineering and Laboratory of Material Physics, Zhengzhou University, Zhengzhou 450052, PR China. E-mail: Jiajf@zzu.edu.cn

have been synthesized, such as nanobelts, nanorods and nanofibers.[4,5,6] With respect to thin- and thick film and their counterparts, one-dimensional ZnO nanostructures which were employed to detect gases have several advantages, for example, surfaces can be functionalized with target-specific receptor species, the operating temperature can be modulated to select the proper surface reactions, and self heated device can be prepared.[7]

As we all known, surface defects and surface adsorption are responsible for gas sensing performance of metal-oxide semiconductor nanostructures, decorating metal oxide nanostructures with catalytic noble metal nanoparticles (NPs) like Pd, Pt, Au, Ag NPs, etc[8,9,10,11]is an efficient way to improve their gas-sensing performance by promoting the activities of their surface defects and surface adsorption.[12,13] It is reported that the decoration of Au, Pd, and Pt NPs on the surface of the metal-oxide semiconductors can improve their sensitivity, selectivity, shorten their response, recovery times and reduce their working temperature.[14,15]

Besides, reliable gas sensing performance of a gas sensor is determined by the properties of the electrode materials such as highly electronic conduction and chemically stableness. Ag, Pd and Pt are the common electrode materials for gas sensors owing to theirs advantages such as low resistivity, excellent thermal and chemical stability.[16] Nonetheless, the high cost limits their application. Conducting metal oxides, such as Indium–tin oxide (ITO), aluminum-doped zinc oxide (AZO), and Lanthanum nickelate ($LaNiO_3$) with resistivity less than $1\times10^{-3}\,\Omega\cdot$cm have been reported.[17,18]These metal oxide materials are much cheaper than Ag or Pt, and their fabrication methods are more compatible with semiconductor manufacturing processes. As a result, $LaNiO_3$ has been widely used as an electrode material in electronic devices such as FeRAM due to its excellent electrical conductivity.[19] For gas sensor applications, reliable gas sensing performance should be expected from gas sensors with $LaNiO_3$ electrodes. However, to the best of our knowledge, the metal oxide gas sensor with conductive metal oxide as electrode material has not been reported.

Precise and reliable handling of these nanostructures is important for bottom-up

assembly of nanodevices, and extensive research efforts have been made to develop one-dimensional metal-oxide nanostructure gas sensors.[20] Dielectrophoresis (DEP) is a facile technique and can be employed to align and manipulate one-dimensional nanostructured materials to the preset locations in fluid for electronic device applications in micro/nanosensors and circuits.[21] In recent years, DEP has been widely exploited for practical applications in the fields of nanotechnology, such as field-effect transistors, molecular electronics, biosensors, and gas sensors, respectively.[22,23,24]

In this work, a novel gas sensor structure is presented. Conducting metal oxide, $LaNiO_3$ films are used to replace Pt, Ag or Pd as the electrodes, and Ag NPs decorated ZnO nanorods are aligned and connected with the electrodes by DEP method. Our results indicate that even though the $LaNiO_3$ has a higher resistivity than Pt, it is suitable for the role of the electrodes for gas sensor applications. Moreover, it is noticeable that Ag NPs decorated ZnO nanorods showed excellent performance for ethanol detection. Details of the growth of Ag NPs decorated one-dimensional nanostructure, the fabrication of novel gas sensor and the characteristics for ethanol vapor detection will be discussed below.

2. Experimental

2.1 Fabrication of $LaNiO_3$ coplanar electrodes

In order to fabricate $LaNiO_3$ coplanar electrodes, $LaNiO_3$ films were prepared by sol-gel method. Lanthanum nitrate and nickel acetate were used as the starting chemicals, and both were dissolved in absolute alcohol solvent with a molar ratio of La:Ni = 1:1. The precursor solution of 0.2 M was then deposited on the quartz glass substrates by repeating the spin-coating cycles to achieve a thickness of about 120 nm. The annealing was carried out at 700 °C for 30 minutes. The resistivity of the $LaNiO_3$ film was measured with a 4-point probe system. The resistivity at room temperature for the $LaNiO_3$ film which was annealed at 700 °C for 30 minutes is 8.2×10^{-4} Ω·cm, which is higher compared with the value of Pt. Subsequently, the $LaNiO_3$ film was

wet-etched using a hydrochloric acid solvent to pattern a coplanar electrode structure with a gap of about 100 μm.

2.2 Preparation of ZnO nanorods

In this work, ZnO nanorods were grown on seeded substrates (regular glass slides) by aqueous chemical method at low-temperature (95 °C). The ZnO seed layer solution was prepared by dissolving 0.02737 g $Zn(CH_3COO)_2 \cdot 2H_2O$ and 0.0175 g hexamethylenetetramine (HMT, $C_6H_{12}N_4$) in 25 ml absolute alcohol under constant stirring. Subsequently, the substrates were soaked into the seed layer solution for 2 seconds, followed by drying with hot air drier. After repeating the procedure for 3~5 times, the substrates were coated by a thin ZnO layer. Then the substrates were transferred into the reaction solution, which was prepared in a beaker by dissolving 0.7425 g $Zn(NO_3)_2 \cdot 6H_2O$ and 0.35 g HMT in 250 ml deionized water. The substrates were placed vertically in the sealed beaker. The beaker was placed in regular water bath at 95 °C for 12 h without disturbance. And then the substrates were taken out of the solution, washed with deionized water for several times and dried in the air. Finally, the white powder (ZnO nanorods) was collected by scraping from the substrates.

2.3 Synthesis of Ag-decorated ZnO nanorods by photochemical deposition (PCD)

In a typical procedure, noble metal decoration was obtained by immersing ZnO nanorods into the silver nitrate-ethanol solution (0.25 mM) and then treated by ultraviolet lamp (365 nm, around 5.3 $mW \cdot cm^{-2}$) irradiation for 30 min. In our research, we used PVP (polyvinylpyrrolidone, average Mw=1,300,000, K=88-96) as a stabilizer by dissolving 32 mg PVP in 30 ml $AgNO_3$ solution and the Ag decorated samples were acquired after ultraviolet photochemical deposition. And then vacuum filtration was used to purify the products, followed by washing with deionized water and absolute ethanol to remove any residual salts and organic materials. Finally, the Ag-decorated ZnO nanorods were obtained by drying in air.

2.4 Assemble all metal-oxide gas sensors based on Ag-decorated ZnO nanorods by DEP method

Before the DEP process, the 2.5 $g \cdot L^{-1}$ suspension of Ag-decorated ZnO nanorods

was acquired by dispersing the nanorods in ethanol via an ultra-sonication process for 5~8 min to yield the required homogeneous distribution of the ZnO nanorods.

The electric field was generated by applying a sinusoidal voltage (0~10 MHz) up to 20 V_{p-p} (peak to peak value) with a function generator (Tektronix AFG3011C). One little drop of the suspension was transferred to the electrode gap by using a pipette and the electric field gradient was applied to pull the nanorods from the solution to electrodes, resulting in the nanorods aligned between the electrode pair.

2.5 Characterization of materials and measurement of gas sensors

X-ray diffraction (XRD) analysis was performed on a PANalytical X' Pert Pro X-ray diffractometer with Cu Kα radiation of 1.5418 Å. Scanning electron microscopy (SEM) images and energy-dispersive X-ray spectroscopy (EDS) spectra were obtained on a JEOL JSM-6700F scanning electron microscope. Transmission electron microscopy (TEM) images were tested on a JEOL JEM-2010 transmission electron microscope. The gas sensing tests were conducted on a gas sensing test system (CGS-1 intelligent test system, Beijing Elite Tech Co. Ltd., China). The PL spectra were performed on a fluorescence spectrometer (Fluorolog-3, HORIBA Scientific) utilizing a 325 nm UV xenon lamp as the excitation source.

3. Results and discussion

3.1 Characteristics of Ag-decorated ZnO nanorods

According to the SEM images of Fig.1 (a) and (b), the micro-morphology of Ag-decorated ZnO nanorods are similar to pure ZnO nanorods. Limited by the resolution of SEM, there is no obvious difference in micro-morphology of ZnO nanorods before and after decorated with Ag NPs by photochemical deposition. In order to observe the distribution of Ag NPs on ZnO nanorods, the TEM images of the Ag-decorated ZnO nanorods are taken and shown in Fig. 1(c) and (d). It is clearly seen that Ag NPs are successfully deposited on the surface of ZnO nanorods, and the average size of Ag NPs is about 30 nm.

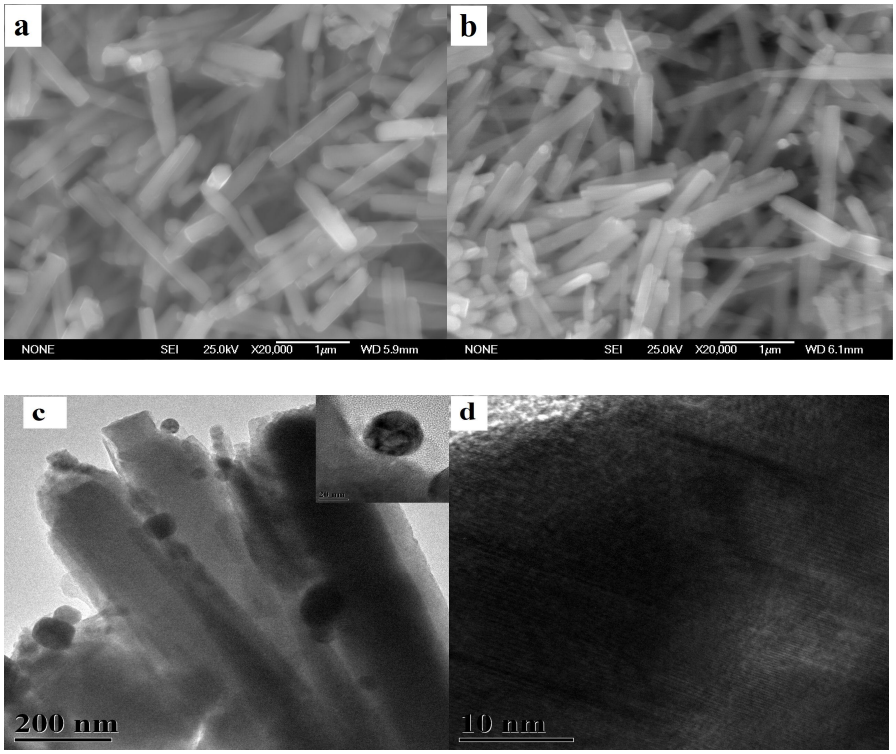

Fig. 1. SEM images of (a) pure ZnO nanorods and (b) Ag-decorated ZnO nanorods. (c) TEM image of Ag-decorated ZnO nanorods and (d) high-magnification TEM of a single Ag nanoparticle.

Fig. 2 shows the XRD patterns of pure ZnO nanorods and Ag NPs decorated ZnO nanorods. Both of the two patterns are in agreement with the standard pattern of ZnO with wurtzite (hexagonal) structure (JCPDS 36-1451). However, though the sample was decorated with Ag NPs by photochemical deposition, there is no obvious diffraction peak attributed to Ag element or compounds in Fig. 2. In combination with the EDS spectra of samples (Fig. 3), which shows the weak existence of Ag in the sample of Ag NPs decorated ZnO nanorods, it indicates that the content of Ag NPs is low on the surface of Ag NPs decorated ZnO nanorod.

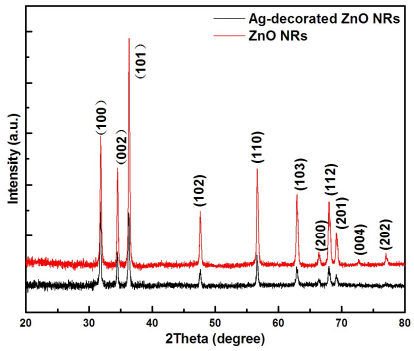

Fig. 2. XRD patterns of pure ZnO nanorods and Ag-decorated ZnO nanorods.

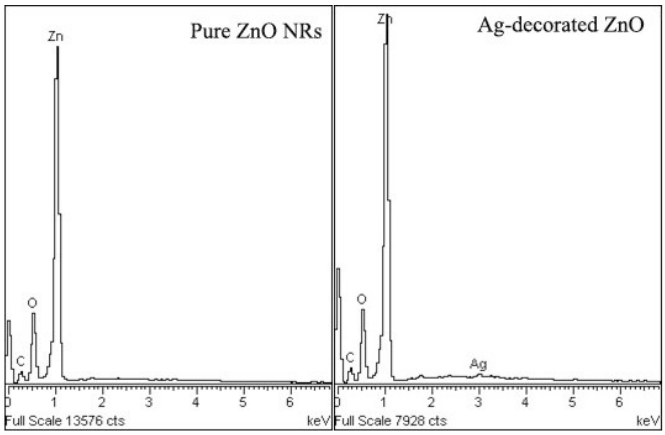

Fig. 3. EDS spectra of pure ZnO nanorods and Ag-decorated ZnO nanorods

Fig. 4 is the room-temperature photoluminescence (PL) spectra of pure and Ag-decorated ZnO NRs. Two UV emissions centering at 384 and 395 nm are observed for pure ZnO NRs. In contrast, for Ag-decorated ZnO NRs, the UV emission is weaker. The UV band emission should be assigned to the direct recombination photogenerated charge carriers (near band-edge emission). [25] A lower photoluminescence intensity means a lower electron–hole recombination rate. The decrease in PL intensity can be ascribed to the electron trapping effect of Ag which act as acceptor species, hindering the recombination of charge carriers on ZnO.[26]

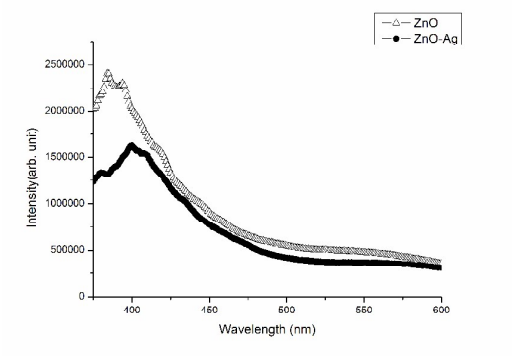

Fig. 4. Photoluminescence spectra of pure and Ag-decorated ZnO NRs

3.2 Dielectrophoresis deposition

In this paper, both the pure ZnO nanorods and Ag-decorated samples were deposited on as-prepared $LaNiO_3$ coplanar electrodes and conventional Ag interdigitated electrodes (alumina substrate, Beijing Elite Tech Co. Ltd., China) via DEP. The dielectrophoretic behavior of ZnO nanorods under the application of electric fields is strongly affected by different dielectrophoretic parameters such as the concentrations of ZnO-suspension, applied voltages, frequencies and processing time. Fig. 5 shows the SEM images of ZnO nanorods assembled by the DEP technique at AC 20 $V_{p\text{-}p}$ and 100 kHz frequency. As can be seen in the figures, the ZnO nanorods have successfully linked together and bridged the gap of two electrodes with a form of pearl-like chain, which is due to the effect called mutual dielectrophoresis.[27]

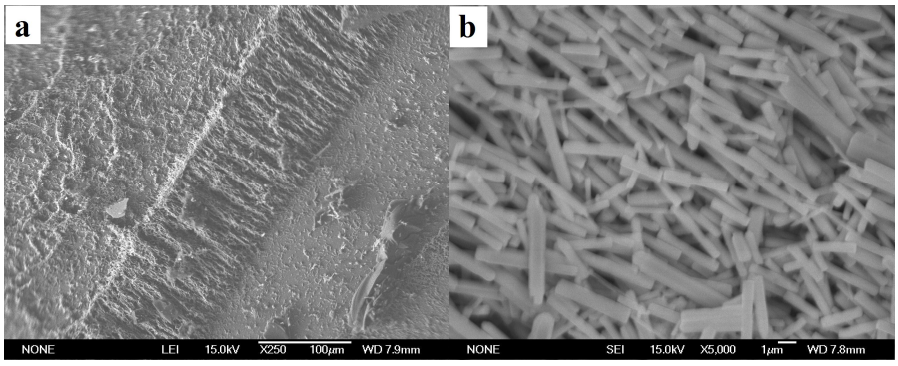

Fig. 5. SEM images of (a) DEP patterns of ZnO nanorods in $LaNiO_3$ electrodes and (b) the chain formations of the aligned ZnO nanorods in the gap of the electrodes.

3.3 Gas sensor performance and sensing mechanisms

For reductive gases (or vapors) in this paper, the response of the sensor is calculated using the expression of $S = R_a/R_g$, where R_a and R_g are the resistances of

samples exposed to air and detected gas, respectively.[28] The response curves of the as-prepared gas sensors upon exposure to ethanol vapor at various working temperature are depicted in Fig. 6. The optimized working temperature of all the samples for ethanol detection is 300 °C, and it is found that the responses are nearly proportional to the increasing concentration of ethanol from 10 to 200 ppm. Moreover, the gas sensing performance of sensors based on $LaNiO_3$ coplanar electrodes is excellent in comparison with the samples based on Ag interdigitated electrodes, which should be due to the chemical stability of $LaNiO_3$ and the formation of favorable ohmic contact between $LaNiO_3$ and ZnO.

In general, when ZnO is exposed to air at a moderate temperature, the oxygen adsorbed on ZnO surface will act as an electron acceptor to form oxygen species (O^- or O^{2-}) by capturing electrons from the conductance band of ZnO, decreasing the electron density in the material and increasing the resistance of ZnO in air ambient (Ra).[29] Once ZnO is exposed to a reductive gas (ethanol for example), the reactions between the reductive gas and oxygen species will result in desorption of adsorbed oxygen, as well as the release of the trapped electrons, which consequently causes a decrease in the resistance of ZnO in a reductive gas ambient (Rg). The related reactions in this procedure can be addressed like this[30]:

$$CH_3CH_2OH + 6O^-(ad) \rightarrow 2CO_2 + 3H_2O + 6e^- \quad (1)$$

According to the response of gas sensor previous defined in this paper, a higher resistance of ZnO in airs ambient (Ra) and a large decrease in resistance of ZnO in a reductive gas ambient (Rg) will indicate higher gas sensitivity. As shown in Fig. 5a and b, compared with pure ZnO nanorods, decoration of Ag NPs on the surface of ZnO nanorods strongly enhanced the ethanol sensing performance.

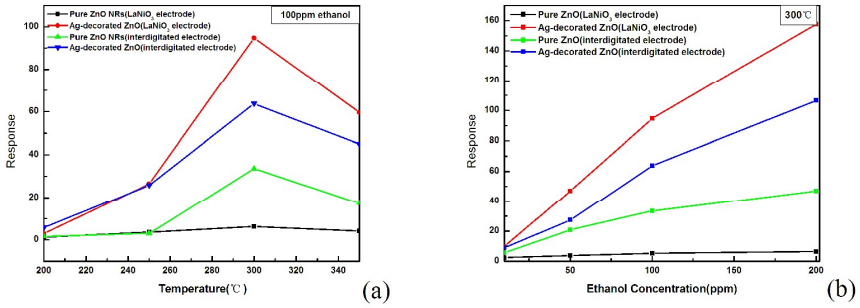

Fig. 6. Gas sensing performance of pure ZnO and Ag-decorated ZnO nanorods: (a) response curves of pure ZnO nanorods and Ag-decorated ZnO nanorods at different temperatures (b) the variation of the response values with different concentration (10, 50, 100, 200 ppm) of ethanol.

In terms of Ag-decorated ZnO, Ag particles can also act as a strong electron acceptor capturing electrons from the conductance band of ZnO, and consequently induce an enlarged surface space charge layer.[31] Moreover, Ag NPs as a catalyzer will activize more adsorbed oxygen dissociated on the surface of ZnO and lead to more electrons trapped from the ZnO. Both of them result in a further increase in the length of depleted layer together with the width and height of the potential barrier near the interface.[32,33] So, the normal ambient resistance of Ag decorated ZnO nanorods in air (Ra) will be even higher than pure ZnO nanorods. And when the sensors are exposed upon a reductive gas, the depleted layer fade away through the reactions between the reductive gas and oxygen species, leading to the decrease in the resistance of sensors.[34] In comparison to the pure ZnO nanorods, there are more trapped electrons released back to the conduction band, more shift of depleted layer length and barrier potential width and height at the contacts.[35] Therefore, the sensors based on Ag NPs decorated ZnO nanorods show the better sensing properties than those based on pure ZnO nanorods. Table 1 shows the sensing performances of Ag NPs decorated ZnO nanorods comparing with those of ZnO nanoparticles, nanorods, brushes, and hollow microspheres in earlier literatures. Accordingly, the response of the Ag NPs decorated ZnO nanorods was much higher and its working temperature was lower. Ag NPs decoration also accelerates the adsorption and desorption rates of gas molecules, thereby resulting in ultrafast response-recovery time of the gas

sensors,[36,37] as shown in Fig. 7.a, b, c and d. Furthermore, among the tested gases (such as ethanol, nitrogen dioxide, acetone, carbon monoxide and methane), the Ag NPs decorated ZnO nanorods have a highest response to ethanol at all temperatures and the same concentration of 100 ppm(Fig. 7e). The selectivity may be attributed to the decoration of Ag. The presence of Ag NPs on the surface of ZnO NRs serves to enhance the C2H5OH oxidation due to a higher oxygen ion-chemisorption on the conductive Ag NPs surfaces. The ethanol oxidation on the Ag NPs leads to the transfer of electrons into the semiconducting ZnO NRs and this is reflected as the change in conductance of sensor.[38]

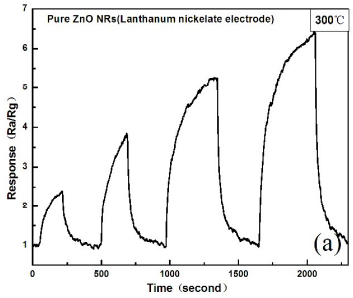

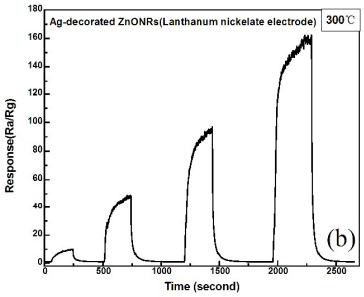

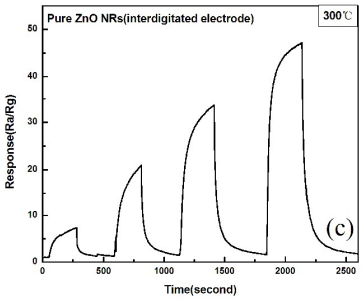

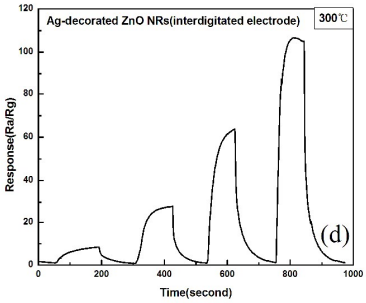

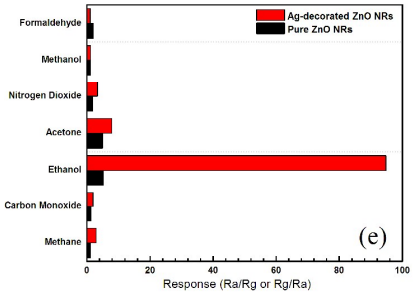

Fig. 7. (a)~(d) Response and recovery curves to (10, 50, 100 and 200 ppm, respectively) ethanol at 300 °C of pure ZnO NRs and Ag-decorated ZnO NRs; (e) Responses to different gases at the concentration of 100 ppm.

Table 1
Comparison of ethanol sensing performances of different ZnO gas sensors.

	Ethanol concentration (ppm)	Working temperature (°C)	Sensor response (S) Rair/Rgas	Reference literatures
ZnO nanoparticles	50	350	~10	[39]
ZnO nanorods	50	330	~9	[40]
ZnO hollow microspheres	50	420	~8.5	[41]
Ag NPs decorated ZnO nanorods	50	300	~24	This work

4. Conclusions

In this work, a simple low-temperature aqueous method was employed to synthesize ZnO nanorods, and the ZnO nanorods were decorated with Ag NPs through photochemical deposition. DEP technique was used to assemble the nanorods into the $LaNiO_3$ electrode gap. The nanorods were well aligned across the gas of the electrodes with a form of pearl-like chain. Owing to the chemical stability of $LaNiO_3$ and the formation of favorable ohmic contact between $LaNiO_3$ and ZnO, the gas sensing performance of sensors based on $LaNiO_3$ coplanar electrodes is excellent in comparison with the samples based on Ag interdigitated electrodes. It proved that the conducting metal oxide $LaNiO_3$ is suitable for the materials of the electrodes for gas sensing applications. Moreover, attributing to Ag nanoparticles decorated on the ZnO nanorod surface, the Ag NPs decorated ZnO nanorods have high selectivity to ethanol in comparison with formaldehyde, methanol, nitrogen dioxide, acetone, carbon monoxide and methane.

References

1 J.G. Lu, P.C. Chang, Z.Y. Fan, *Mater. Sci. Eng.*, *R*, 2006, 52, 49.

2 D.C. Look, *Mater. Sci. Eng., B*, 2001, 80, 383.

3 C.G. Van de Walle, *Physica B: Condens. Matter.*, 2001, 308, 899.

4 X.R. Qu , W. Wang, W. Liu, Z.H. Yang, X.M. Duan, D.C. Jia, *Mater. Sci. Semicond. Process.*, 2011, 14, 241.

5 E.S. Jang, J.H. Won, Y.W. Kim, Z. Cheng, J.H. Choy, *J. Solid State Chem.*, 2010, 183, 1835.

6 D.S. Kang, H.S. Lee, S.K. Han, V. Srivastava, E.S. Babu, S.K. Hong, M.J. Kim, J.H. Song, J.H. Song, H.J. Kim, D.J. Kim, *J. Alloys Compd.*, 2011, 509, 5137.

7 E. Comini, C. Baratto, I. Concina, G. Faglia, M. Falasconi, M. Ferroni ,V. Galstyan, E. Gobbi, A. Ponzoni, A. Vomiero, D. Zappa, V. Sberveglieri, G. Sberveglieri, *Sens. Actuators, B*, 2013, 179, 3.

8 C.M. Chang, M.H. Hon, and I.C. Leu, *Appl. Mater. Inter.*, 2013, 5, 135.

9 J. Guo, J. Zhang, M. Zhu, D. X. Ju, H. Y. Xu, B. Q. Cao, *Sens. Actuators, B*, 2014, 199, 339.

10 M.A. Lim, Y.W. Lee, H.S. Woo, I. Park, *Nanotech.*, 2011, 22, 035601.

11 P. Eunyu, K. O. Seok, P. S. Joo, L.J. Seo, Y. Sunah, J. Jyongsik, *J. Mater. Chem.*, 2012, 22, 1521.

12 D.D. Frolov, Y.N. Kotovshchikov, I.V. Morozov, A.I. Boltalin, A.A. Fedorova, A.V. Marikutsa, M.N. Rumyantseva, A.M. Gaskov, E.M. Sadovskaya, A.M. Abakumov, *J. Solid State Chem.*, 2012, 186, 1.

13 A.S.M. Iftekhar Uddin, Duy-Thach Phan, Gwiy-Sang Chung, *Sens. Actuators, B*, 2015, 207, 362.

14 S. Nandan, G.R. Kumar, L.P. See, *Appl. Mater. Inter.*, 2011, 3, 2246.

15 Y. Masayoshi, K. Tetsuya, S. Kengo, *Appl. Mater. Inter.*, 2012, 4, 4231.

16 S. Capone, M. Epifani, L. Francioso, S. Kaciulis, A. Mezzi, P. Siciliano, A.M. Taurino, *Sens. Actuators, B*, 2006, 115, 396.

17 T. Minami, *Semicond. Sci. Technol.*, 2005, 20, S35.

18 C. R. Cho, D. A. Payne and S. L. Cho, *Appl. Phys. Lett.*, 1997, 71, 3013.

19 K.T. Kim, C.I. Kim, J.G. Kim, G.H. Kim, *Thin Solid Films*, 2007, 515, 8082.

20 N. Chartuprayoon, M.L. Zhang, W.Bosze, Y.H. Choa, N.V. Myung, *Biosens. Bioelectron.*, 2015, 63, 432.

21 W. J. Liu, J. Zhang, L.J. Wan, K.W. Jiang, B.R. Tao, H.L. Li, W.L. Gong, X.D. Tang, *Sens. Actuators, B*, 2008, 133, 664.

22 S.Y. Lee, A. Umar1, D. Suh, J.E. Park, Y.B. Hahn, J.Y. Ahn, S.K. Lee, *Physica E*, 2008, 40, 866.

23 K.S. Vasu, B. Chakraborty, S. Sampath, A.K. Sood, *Solid State Commun.*, 2010, 150, 1295.

24 J. Suehiro, N. Sano, G. B. Zhou, H. Imakiire, K. Imasaka, M. Hara, *J. Electrostat.*, 2006, 64, 408.

25 W. Bai, K. Yu, Q.X. Zhang, F. Xu, D.Y. Peng, Z.Q. Zhu, *Appl. Surf. Sci*., 2007, 253, 6835.

26 Z. F. Zhang, H. R. Liu, H. Zhang, H. L. Dong, X. G. Liu, H. S. Jia, B. S. Xu, *Superlattices Microst*., 2014, 65, 134.

27 M.P. Hughes, *Nanoelectromechanics in engineering and biology* (book), CRC Press, Washington D.C, 2003.

28 X. Z. Wang, S. Qiu, C. Z. He, G. X. Lu, W. Liu and J. R. Liu, *RSC Adv.*, 2013, 3, 19002.

29 J.Q. Xu, Y.P. Chen, D.Y. Chen, J.N. Shen, *Sens. Actuators, B*, 2006, 113, 526.

30 Z.X. Yang, Y. Huang, G.N. Chen, Z.P. Guo, S.Y. Cheng, S.Z. Huang, *Sens. Actuators, B*, 2009, 140, 549.

31 R. Georgekutty, M.K. Seery, S.C. Pillai, *J. Phys. Chem. C,* 2008, 112, 13563.

32 Q. Xiang, G. F. Meng, Y. Zhang, J. Q. Xu, P. C. Xu, Q. Y. Pan, W. J. Yu, *Sens. Actuators, B*, 2010, 143, 635.

33 H. R. Liu, Y. C. Hu, Z. X. Zhang, X. G. Liu, H. S. Jia, B. S. Xu, *Appl. Surf. Sci.,* 2015, 355, 644.

34 X. G. San, G. S. Wang, B. Liang, Y. M. Song, S. Y. Gao, J. S. Zhang, F. L. Meng, *J. Alloys Comp.*, 2015, 622, 73.

35 H. Li, J. Q. Xu, Y. H. Zhu, X. D. Chen, Q. Xiang, *Talanta*, 2010, 82, 458.

36 C.M. Chang, M.H. Hon, I.C. Leu, *RSC Adv.*, 2012, 2, 2469.

37 L. Liao, H. B. Lu, J. C. Li , H. He , D. F. Wang, D. J. Fu, and C. Liu, *J. Phys. Chem. C*, 2007, 111, 1900.

38 W. Jin, S. L. Yan, W. Chen, S. Yang , C. X. Zhao, Y. Dai, *Funct. Mater. Lett.*, 2014, 7, 145031.

39 J. Xu, J. Han, Y. Zhang, Y.A. Sun, B. Xie, *Sens. Actuators, B*, 2008, 1, 334.

40 J. Xu, Y. Chen, Y. Li, J. Shen, *J. Mater. Sci.*, 2005, 11, 2919.

41 Y. Tian, J. Li, H. Xiong, J. Dai, *Appl. Surf. Sci.*, 2012, 22, 8431.